Influence Rate of Semiconductor ON-Voltage in Inverter Circuit on Iron Loss Inside a Non-Oriented Electrical Steel Sheet

Shunya Odawara and Keisuke Fujisaki

Department of Advanced Science and Technology, Toyota Technological Institute, Nagoya 4688511, Japan

We calculate an iron loss attributed to semiconductors ON-voltages in an inverter circuit and reveal influence rate of the ON-voltages on whole iron loss. In our previous work, it has been revealed by inverter excitation that the ON-voltages make minor loops in magnetic hysteresis of magnetic material and the loops affect iron loss characteristics. In this paper, it is investigated by a factor analysis how much the on-voltage has an influence on iron loss, quantitatively. We separate whole iron loss caused in a non-oriented electrical steel sheet into three losses: loss by the ON-voltage, loss by fundamental component, and loss by inverter carrier. The rates of these losses are evaluated under several conditions of single-phase pulse width modulation inverter excitation, and the results show that the proportion of loss by ON-voltages is up to around 10% depending on inverter excitation parameter: fundamental frequency, carrier frequency, modulation index, and magnetic flux density.

Index Terms—**Factor analysis, iron loss, non-oriented electrical steel sheet, ON-voltage, single-phase pulse width modulation (PWM) inverter excitation.**

NOMEMCLATURE

H	Magnetic field intensity.
B	Magnetic flux density.
$B_{\max}$	Maximum magnetic flux density in electrical steel sheet.
f_o	Fundamental frequency.
f_c	Carrier frequency for inverter excitation.
m	Modulation index for inverter excitation.
V_{dc}	dc voltage for inverter excitation.
V_{ON}	Whole ON-voltage in inverter circuit.
V_s	ON-voltage of switching IGBT in inverter circuit.
V_d	ON-voltage of freewheel diode in inverter circuit.
W_{fe}	Whole iron loss caused in electrical steel sheet.
W_{ON}	Iron loss attributed to ON-voltage of power semiconductor in inverter circuit.
W_{fo}	Iron loss attributed to fundamental component in inverter excitation.
W_{fc}	Iron loss attributed to inverter carrier.
σ	Electrical conductivity of electrical steel sheet.
d	Thickness of electrical steel sheet.
ρ	Volume density of electrical steel sheet.
κ	Anomaly factor to consider anomaly eddy current.
R	Equivalent resistance to express eddy current loss in Cauer circuit.
L	Equivalent inductance to express magnetic flux in Cauer circuit.

I. INTRODUCTION

ELECTRICAL steel sheets are used widely as iron cores of electrical motors, transformers, and reactors. These electrical apparatus are driven by various driving conditions (e.g., a sinusoidal excitation by commercial frequency or an inverter excitation to generate variable voltage and frequency). In this case, the electrical steel sheets are magnetized by the excitation conditions. Many researchers [1]–[14] have investigated the magnetic properties of steel sheets under various excitation conditions. As a consequence of the investigations on inverter excitation, they have reported that the inverter excitation causes minor loops in magnetic hysteresis and these minor loops cause iron loss increase. The formation of minor loops depends on excitation conditions such as carrier frequency and modulation index. Furthermore, in [15]–[17], it has been revealed that ON-voltages of power semiconductor devices in inverter circuit also affect the shape of minor loops. In brief, ON-voltages characteristics should affect iron loss characteristics of a magnetic material. In conventional research, there are no reports about influence rate of ON-voltages on iron loss. To clarify, the influence rate will lead suitable device selection for low iron loss on an inverter excitation condition.

As a specific example, we have observed impact of the ON-voltages on iron loss characteristics [15]–[17]. In [16], the iron loss is increased about 20% by using the semiconductor having about 20 times large ON-voltage, in spite of the same inverter excitation condition. On the other hand, however, the results with inverse tendency are also obtained in [17]: the iron loss is not increased even if the semiconductors having different ON-voltages are used. Therefore, as a foothold to clarify the strange phenomenon, we investigate the influence of ON-voltages in detail.

First of all, as an initial study, we separate an inverter iron loss into three losses by a numerical analysis in order to evaluate the influence rate of ON-voltage. The three losses are the losses caused by fundamental component, inverter carrier, and semiconductor ON-voltage. An experimental investigation will be carried out as a future work. When the numerical analysis is carried out, the magnetic material property and the semiconductor property should be considered at the same time because magnetic hysteresis has to be affected by semiconductor ON-voltage. There are some modelings for magnetic

Manuscript received February 24, 2017; revised July 2, 2017 and October 2, 2017; accepted January 16, 2018. Date of publication February 23, 2018; date of current version April 17, 2018. Corresponding author: S. Odawara (e-mail: sodawara@mail.kitami-it.ac.jp).

Color versions of one or more of the figures in this paper are available online at http://ieeexplore.ieee.org.

Digital Object Identifier 10.1109/TMAG.2018.2796071

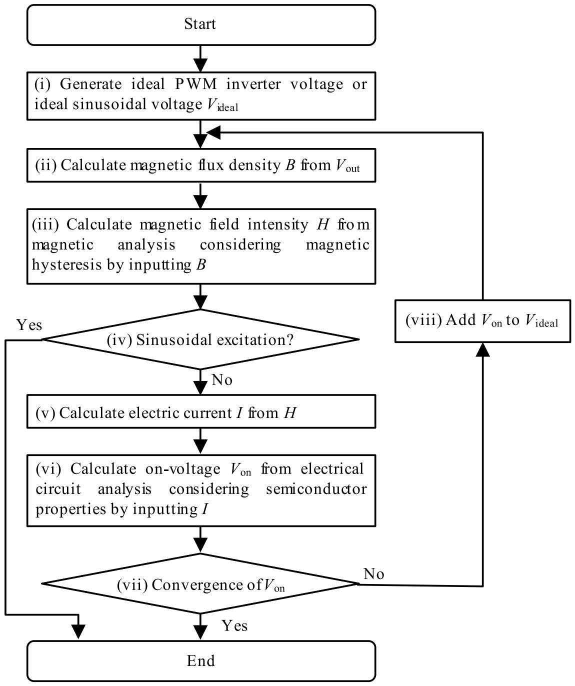

Fig. 1. Flowchart of numerical calculation to take into account power semiconductor property and magnetic hysteresis property.

hysteresis property [18]–[23] or for semiconductor property with electrical circuit [24]–[26]. Although the analysis can be carried out by coupling an inverter circuit analysis with a magnetic hysteresis analysis by finite-element method (FEM) [26], it becomes complicated calculation and takes calculation costs. Therefore, the numerical technique proposed in [27] is used for the analysis. This technique can consider the magnetic property and the semiconductor property iteratively, without complicated coupling and FEM. In fact, the calculation time of one case is about 5 s.

In this paper, first, we explain the numerical technique to consider both properties, because we extend the technique from [27] so that more high frequency can be evaluated adequately, and [27] is written in Japanese. Next, it is described how to separate the iron loss by inverter excitation into three losses. Finally, by using a non-oriented electrical steel sheet and a single-phase PWM inverter, we reveal the impact of ON-voltage under several exciting conditions changing fundamental frequency, carrier frequency, modulation index, and maximum flux density in the steel sheet.

II. Analysis Method to Consider Magnetic Hysteresis and Semiconductor ON-Voltage

Magnetic properties under inverter excitation are obtained from a numerical analysis flow, as shown in Fig. 1. It is possible to reflect semiconductors properties in inverter circuit considered at procedure (vi) to magnetic hysteresis properties of magnetic material considered at procedure (iii).

In procedure (i), we generate an ideal output voltage waveform of inverter excitation or sinusoidal excitation on determined conditions. In procedure (ii), a waveform of magnetic flux density is obtained from time integration of the ideal voltage. In procedure (iii), a waveform of magnetic field intensity considering magnetic hysteresis property is obtained from magnetic analysis using play model with Cauer circuit. In procedure (iv), if the case of sinusoidal excitation, the analysis is finished, else the process goes to procedure (v). In procedure (v), a current waveform is obtained from the magnetic field intensity. In procedure (vi), we carry out a circuit analysis by inputting the current waveform, and ON-voltages of semiconductors are obtained. In procedure (vii), if the ON-voltages do not change from those of one flow cycle before, the analysis is finished, else as a procedure (viii), the ON-voltages are added to ideal output voltage made in procedure (i).

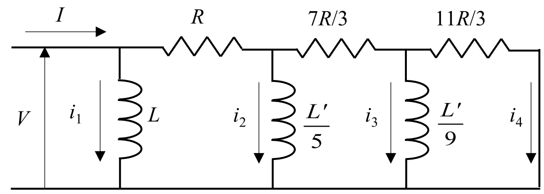

Fig. 2. Cauer circuit ($n = 3$) to express up to 200 kHz.

We explain the procedures (iii) and (vi) in detail. First, in procedure (iii), play model is used to consider magnetic hysteresis property, and play model can express a dc magnetic hysteresis [23]. Therefore, influence of eddy current is considered by Cauer circuit theory [28], [29]. Cauer circuit shown in Fig. 2 can express the eddy current effects and skin effects by high inverter carrier frequency, without FEM. The circuit can convert distributed constant circuit into lumped constant circuit. For example, first inductance L relates to main magnetic flux in steel sheet and first resistance R relates to eddy current by the main magnetic flux. When frequency is high, the eddy current expressed by R makes new reaction magnetic flux. The new magnetic flux is expressed by next inductance $L'/5$. Therefore, expressible frequency depends on the rank n of the circuit. The circuit of rank 3 can express up to 100 kHz. In Section IV, we investigate by using up to 10 kHz carrier frequency. Therefore, in order to express up to 10 times harmonics adequately, we choose the circuit of rank 3. Incidentally, the circuit of rank 2 can express up to 20 kHz. In this magnetic analysis, rotational magnetic flux cannot be expressed because only magnetic flux flowing one way can be expressed. However, the evaluation of one direction is enough to evaluate magnetic material property on ON-voltage as an initial study.

By solving the circuit equations, we can obtain magnetic field intensity taking account of magnetic hysteresis from magnetic flux density. The circuit equations are shown as follows:

$$V = L\frac{di_1}{dt} \tag{1}$$

$$V = R(i_2 + i_3 + i_4) + \frac{L'}{5}\frac{di_2}{dt} \tag{2}$$

$$V = R(i_2 + i_3 + i_4) + \frac{7}{3}R(i_3 + i_4) + \frac{L'}{9}\frac{di_3}{dt} \tag{3}$$

$$V = R(i_2 + i_3 + i_4) + \frac{7}{3}R(i_3 + i_4) + \frac{11}{3}Ri_4 \tag{4}$$

$$R = \frac{12}{\kappa\sigma d^2}. \tag{5}$$

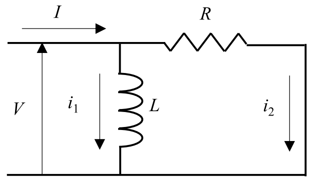

Fig. 3. Cauer circuit ($n = 1$) to express up to 400 Hz.

In Cauer circuit, V and I correspond to dB/dt and H, respectively. Therefore, we can perform the permutation of variables. Because main magnetic field intensity in steel sheet is obtained from the whole H $(= H_1 + H_2 + H_3 + H_4)$, deformation of the equations about H is carried out as follows:

$$H^k(B^k) = H_1^k + H_2^k + H_3^k + H_4^k \tag{6}$$
$$H_2^k = C_1 H_4^k + C_2 + H_2^{k-1} \tag{7}$$
$$H_3^k = C_3 H_4^k + H_3^{k-1} \tag{8}$$
$$H_4^k = \frac{1}{C_4}\{5(B^k - B^{k-1}) - C_5\} \tag{9}$$
$$C_1 = \frac{1}{9L'}\{105R\Delta t(C_3+1) + 5L'C_3\} \tag{10}$$
$$C_2 = \frac{105}{9L'}R\Delta t\left(H_3^{k-1}\right) \tag{11}$$
$$C_3 = \frac{99}{L'}R\Delta t \tag{12}$$
$$C_4 = 5R\Delta t(C_1 + C_3 + 1) + L'C_3 \tag{13}$$
$$C_5 = 5R\Delta t\left(C_2 + H_2^{k-1} + H_3^{k-1}\right) + L'C_2 \tag{14}$$

where Δt is the time division, H_1 is calculated by scalar play model. κ and L' are the anomaly factor to express anomaly eddy current loss and the equivalent inductance to express magnetic flux by eddy current. L has (′) to discern from the first L. Although the first L is non-linear inductance to express magnetic hysteresis, L' is linear inductance and the attitude is enough to express high frequency [30].

κ and L' are unknown values, and we should determine both the values. However, it is hard to determine the two values at the same time. Therefore, first, only κ is determined by using circuit of rank 1 as shown in Fig. 3. This circuit can express up to 400 Hz and it does not have L'. To determine κ, sinusoidal excitation is used. In this case, although the anomaly eddy current loss by carrier frequency cannot be considered, we neglect it for simplicity. In the circuit of rank 1, as with the above equations, H^k is calculated by the following equations:

$$H^k(B^k) = H_1^k + H_2^k \tag{15}$$
$$H_2^k = \frac{B^k - B^{k-1}}{R\Delta t}. \tag{16}$$

where κ is determined by fitting so that the analyzed iron loss becomes the same as measured iron loss on sinusoidal excitation. The core material of measured steel sheet is non-oriented material (35H300). The iron losses are obtained from the following equation:

$$W_{\mathrm{fe}} = \frac{f_o}{\rho}\int \mathrm{HdB} \tag{17}$$

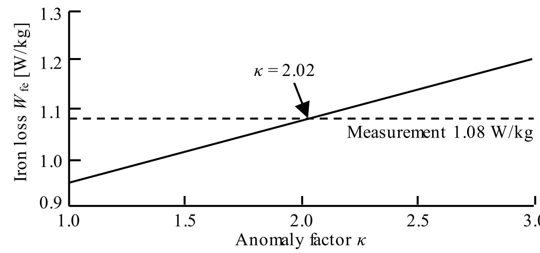

Fig. 4. Relation between κ and W_{fe} (sinusoidal excitation: 50 Hz and $B_{\max} = 1$ T, 35H300).

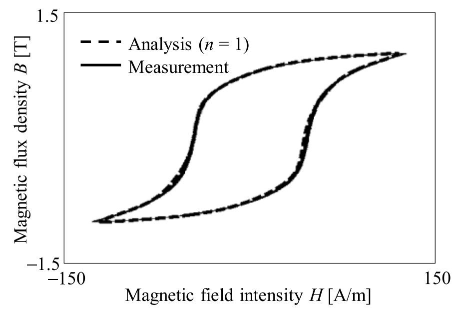

Fig. 5. Analyzed and measured B–H curves of 35H300 on 50 Hz sinusoidal excitation.

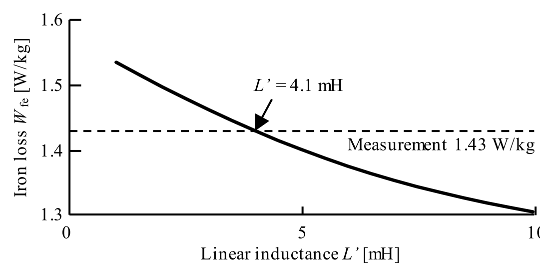

Fig. 6. Relation between L' and W_{fe} (single-phase PWM inverter excitation: $f_o = 50$ Hz, $f_c = 1$ kHz, $m = 0.5$, and $B_{\max} = 1$ T, 35H300).

where B and H are obtained from procedures (ii) and (iii) in Fig. 1, respectively. For example, Fig. 4 shows the relation between κ and W_{fe} on 50 Hz sinusoidal excitation, and it indicates κ should be determined in 2.02. In the factor analysis mentioned below, the value is invariable on the same fundamental frequency condition. Fig. 5 shows the B–H curves by the analysis and measurement on 50 Hz sinusoidal excitation. The analyzed B–H curve expresses the measured one, adequately.

L' is determined from circuit of rank 3 so that the analyzed iron loss becomes the same as measured iron loss under single-phase PWM inverter excitation. For example, Fig. 6 shows the relation between L' and W_{fe} on the following conditions: fundamental frequency 50 Hz, carrier frequency 1 kHz, modulation index 0.5, and maximum flux density 1 T. Fig. 6 indicates L' should be determined in 4.1 mH. L' is calculated on each excitation conditions in the factor analysis. Fig. 7 shows L' when carrier frequency and modulation index are changed.

Next, in procedure (vi), ON-voltages of semiconductors in inverter circuit are calculated from circuit analysis. In case of inverter excitation, minor loops are caused by voltage drop

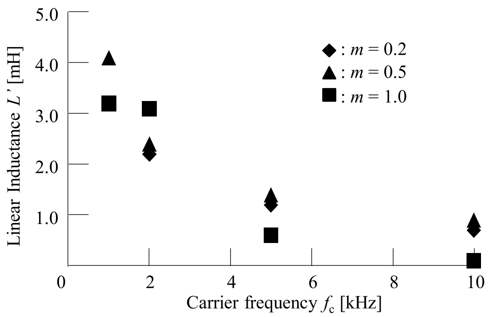

Fig. 7. Relation of L' and carrier frequency f_c and modulation index m. ($f_o = 50$ Hz and $B_{\max} = 1$ T, 35H300).

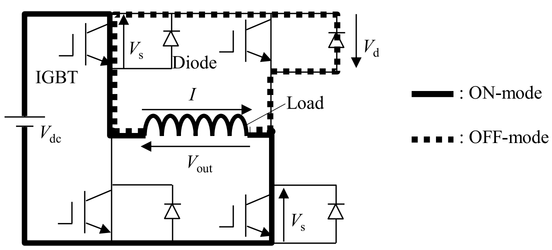

Fig. 8. Current flows in single-phase inverter circuit.

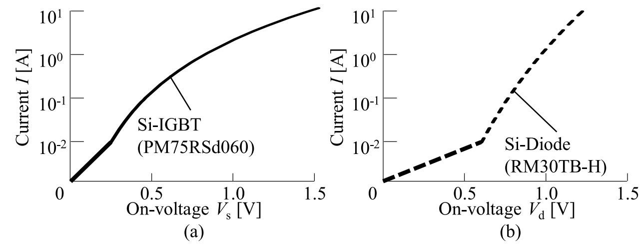

Fig. 9. I–V characteristics of (a) Si-IGBT and (b) Si-Diode.

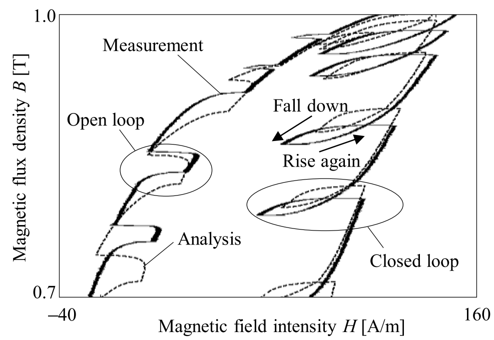

Fig. 10. Analyzed and measured B–H curves of 35H300 near maximum flux density under inverter excitation ($f_o = 50$ Hz, $f_c = 1$ kHz, $m = 0.5$, and $B_{\max} = 1$ T).

at on-resistance of the semiconductors: switching devices and freewheel devices. This voltage drop is called "ON-voltage." In this paper, impact of dead time and a rise time of semiconductor are neglected to evaluate impact of only ON-voltage. The circuit equations of single-phase inverter shown in Fig. 8 are expressed as follows:

$$V_{\mathrm{dc}} = V_s + V_{\mathrm{out}} + V_s \tag{18}$$

$$0 = V_d + V_{\mathrm{out}} + V_s. \tag{19}$$

Equations (18) and (19) indicate ON-mode and OFF-mode, respectively. V_s and V_d are the ON-voltage of switching Si-IGBT (PM75RSd060) and the ON-voltage of freewheel Si-Diode (RM30TB-H) obtained from current–voltage characteristics, as shown in Fig. 9. These semiconductors are attached in commercial inverter (MWINV-9R122B) used for our measurement. Thus, the whole ON-voltages V_{ON} of each mode is obtained as follows:

$$V_{\mathrm{ON}}^{\mathrm{ON\text{-}MODE}} = \pm 2V_s \tag{20}$$

$$V_{\mathrm{ON}}^{\mathrm{OFF\text{-}MODE}} = \pm (V_d + V_s) \tag{21}$$

where "$\pm$" is decided by the direction of current flow. In particular, the ON-voltage of OFF-mode makes minor loops. When V_{out} on OFF-mode is negative and V_{out} on ON-mode is positive, magnetic flux density B falls down and rises again from procedure (ii). As a result, minor loops are depicted in magnetic hysteresis, as shown in Fig. 10.

Fig. 10 shows the analyzed B–H curve and measured B–H curve near maximum flux density $B_{\max}$. B–H curve from analysis depicts suitable minor loops: open loops and closed loops. Some differences of the waveforms are caused by neglecting dead time and a rise time of semiconductor.

TABLE I

LOSS COMPONENTS ON EACH CALCULATION

Calc. no.	Loss	Excitation condition	By Fundamental component	By inverter Carrier	By semiconductor On-voltage
1	$W_{\mathrm{fe}}^{(1)}$	Sinusoidal	○	×	×
2	$W_{\mathrm{fe}}^{(2)}$	Inverter ($V_{\mathrm{on}} = 0$)	○	○	×
3	$W_{\mathrm{fe}}^{(3)}$	Inverter ($V_{\mathrm{on}} \neq 0$)	○	○	○

III. METHOD FOR FACTOR ANALYSIS

To evaluate the influence rate of ON-voltage, we separate whole iron loss into three iron losses. The three losses W_{fo}, W_{fc}, and W_{ON} are caused by fundamental component, inverter carrier, and semiconductor ON-voltages, respectively. From the three losses, we evaluate the proportion of W_{ON} on whole iron loss. In this section, the separation methods are described under an inverter exciting condition: single-phase, fundamental frequency 50 Hz, carrier frequency 1 kHz, modulation index 0.5, and maximum flux density 1 T.

An excited magnetic material is non-oriented electrical steel sheet 35H300: thickness $d = 0.35$ mm, conductivity $\sigma = 1.923 \times 10^6$ S/m, and volume density $\rho = 7650$ kg/m^3. The exciting direction is one way without rotational magnetic flux. We carry out three patterns calculations to obtain the three losses, by changing exciting conditions as shown in Table I.

First, iron loss $W_{\mathrm{fe}}^{(1)}$ is calculated by sinusoidal excitation of 50 Hz and $W_{\mathrm{fe}}^{(1)}$ indicates W_{fo} as follows:

$$W_{\mathrm{fo}} = W_{\mathrm{fe}}^{(1)}. \tag{22}$$

Fig. 11 shows the waveforms of voltage, current, magnetic flux density, and magnetic field intensity. In this condition, since $W_{\mathrm{fe}}^{(1)}$ becomes 1.077 W/kg and W_{fo} is also 1.077 W/kg.

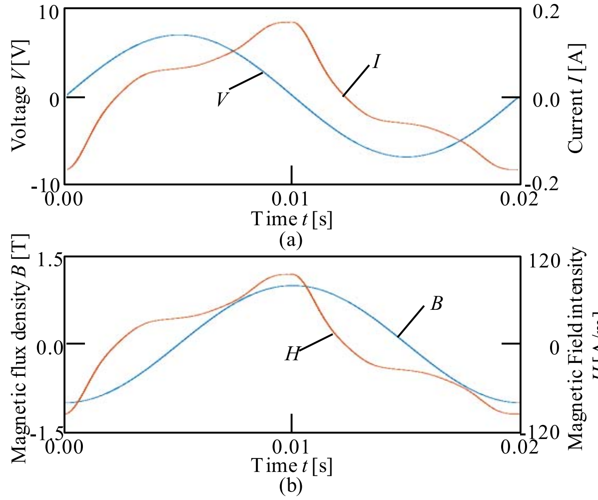

Fig. 11. Waveforms under sinusoidal excitation. (a) Voltage and current. (b) Magnetic flux density and magnetic field intensity.

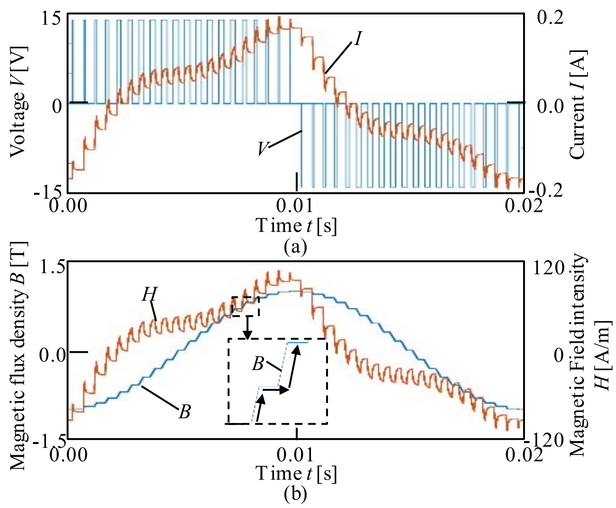

Fig. 12. Waveforms under inverter excitation without ON-voltage component. (a) Voltage and current. (b) Magnetic flux density and magnetic field intensity.

Next, iron loss $W_{\mathrm{fe}}^{(2)}$ is calculated under inverter excitation without ON-voltage: procedures (vi) and (vii) are skipped in Fig. 1. $W_{\mathrm{fe}}^{(2)}$ is composed of W_{fo} and W_{fc}. Therefore, only W_{fc} is obtained by subtracting $W^{(1)}$ from $W_{\mathrm{fe}}^{(2)}$, as the following equation:

$$W_{\mathrm{fc}} = W_{\mathrm{fe}}^{(2)} - W_{\mathrm{fe}}^{(1)}. \tag{23}$$

Since $W_{\mathrm{fe}}^{(2)}$ becomes 1.353 W/kg and W_{fc} is 0.276 W/kg. Figs. 12 and 13 show each waveform and B–H curves. The hatching bulge parts in Fig. 13 indicate W_{fc}.

Finally, $W_{\mathrm{fe}}^{(3)}$ is calculated under inverter excitation with ON-voltage. $W_{\mathrm{fe}}^{(3)}$ is whole iron loss and includes W_{fo}, W_{fc}, and W_{ON}. Therefore, W_{ON} is obtained from the following equation:

$$W_{\mathrm{ON}} = W_{\mathrm{fe}}^{(3)} - W_{\mathrm{fe}}^{(2)}. \tag{24}$$

Since $W_{\mathrm{fe}}^{(3)}$ becomes 1.409 W/kg and W_{ON} is 0.056 W/kg. Figs. 14 and 15 are waveforms and B–H curves. The minor loops of hatching parts in Fig. 15 are caused by ON-voltage.

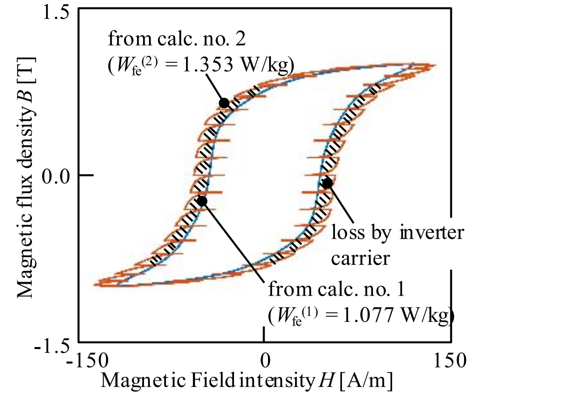

Fig. 13. B–H curves obtained from calculations 1 and 2 shown in Table I.

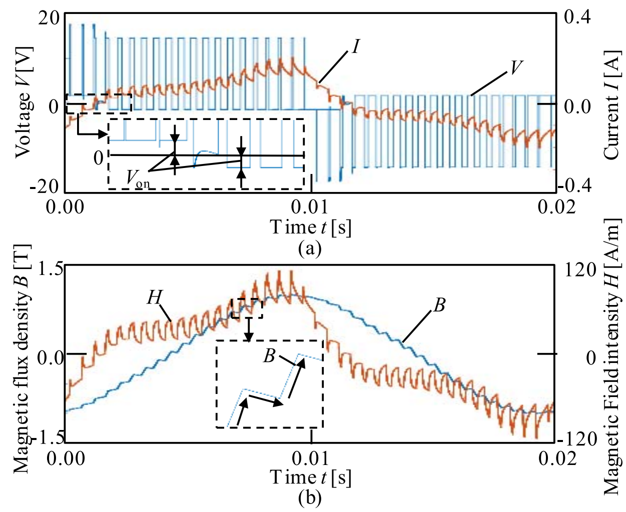

Fig. 14. Waveforms under inverter excitation with ON-voltage component. (a) Voltage and current. (b) Magnetic flux density and magnetic field intensity.

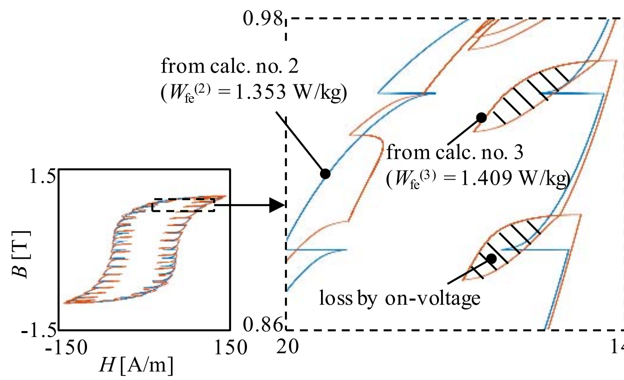

Fig. 15. B–H curves obtained from calculations 2 and 3 shown in Table I.

Table II shows each iron loss value and the percentage on whole iron loss. In this condition, the proportion of W_{ON} is 4%.

IV. Factor Analyses of Iron Loss Under Several Inverter Excitation Conditions

Fig. 16 shows the carrier frequency characteristics and the modulation index characteristics of iron loss under

TABLE II

EACH LOSS ON $f_o = 50$ Hz, $f_c = 1$ kHz, $m = 0.5$, AND $B_{\max} = 1$ T

Factors	W_{fo}	W_{fc}	W_{on}
Loss [W/kg]	1.077	0.276	0.056
Percentage [%]	76.4	19.6	4.0

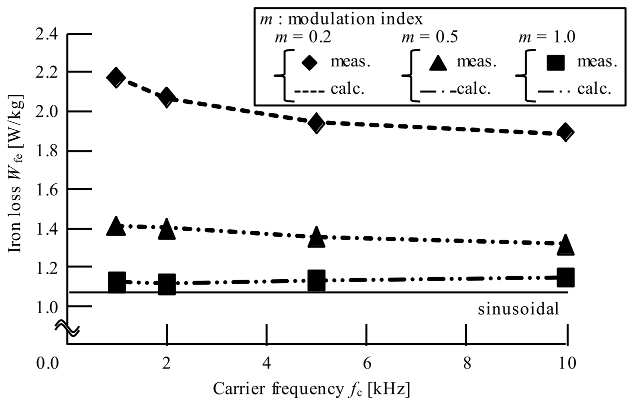

Fig. 16. Carrier frequency and modulation index characteristics of iron loss under inverter excitation ($B_{\max} = 1$ T, 35H300).

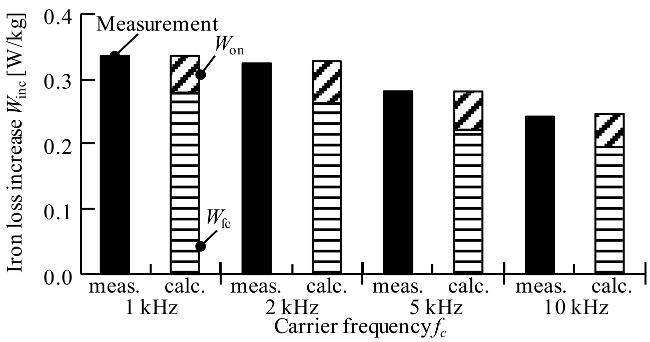

Fig. 17. Iron loss increase on each carrier frequency ($f_o = 50$ Hz, $m = 0.5$, and $B_{\max} = 1$ T).

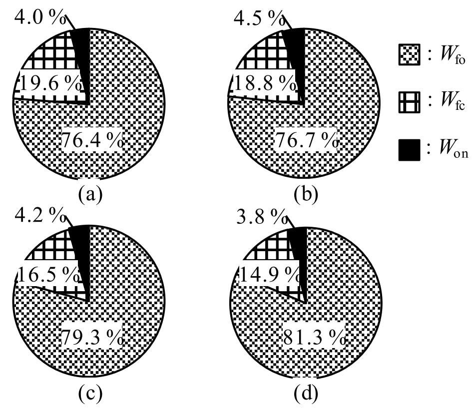

Fig. 18. Loss percentages on carrier frequency (a) 1, (b) 2, (c) 5, and (d) 10 kHz ($f_o = 50$ Hz, $m = 0.5$, and $B_{\max} = 1$ T).

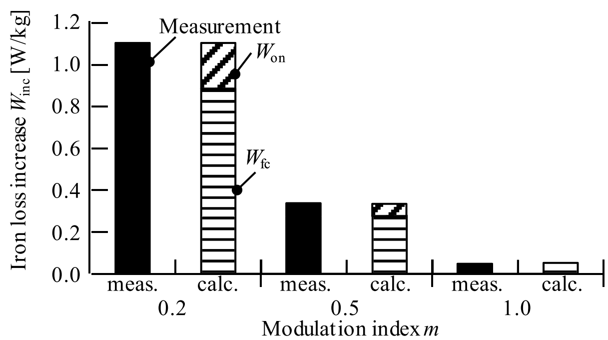

Fig. 19. Iron loss increase on each modulation index ($f_o = 50$ Hz, $f_c = 1$ kHz, and $B_{\max} = 1$ T).

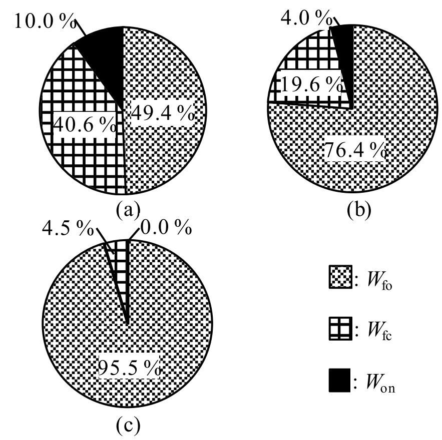

Fig. 20. Loss percentages on modulation index (a) 0.2, (b) 0.5, and (c) 1 ($f_o = 50$ Hz, $f_c = 1$ kHz, and $B_{\max} = 1$ T).

single-phase inverter excitation. The calculated results are the same as the measured results because parameter fitting mentioned in Section II is carried out. It is known that the iron loss is changed by carrier frequencies and modulation indexes even if the same inverter is used. Therefore, the proportion of three iron losses obtained in the preceding section should be evaluated by changing excitation conditions: fundamental frequency, carrier frequency, modulation index, and maximum magnetic flux density.

First, carrier frequency f_c or modulation index m, which are peculiar parameter of inverter excitation, are changed. When f_c is changed, m is set to constant value 0.5. When m is changed, f_c is set to 1 kHz. In both case, the fundamental frequency f_o and the maximum magnetic flux density $B_{\max}$ are set to 50 Hz and 1 T, respectively.

Fig. 17 shows the iron loss increase from iron loss of sinusoidal excitation by variation of carrier frequency. W_{fo} is constant with 1.077 W/kg. Fig. 18 shows the proportion of three losses. In Fig. 17, W_{ON} is almost constant with f_c. W_{ON} is caused by OFF-mode ON-voltage shown in Fig. 14(a). The OFF-mode time for one carrier period becomes small in high carrier frequency. However, total OFF-mode time for one fundamental period does not change by carrier frequency. Therefore, W_{ON} is hardly affected by carrier frequency. The proportion of W_{ON} is also almost constant by carrier frequency.

Figs. 19 and 20 show the iron loss increase and the proportion by variation of modulation index corresponding to Figs. 17 and 18. W_{fo} is also constant with 1.077 W/kg.

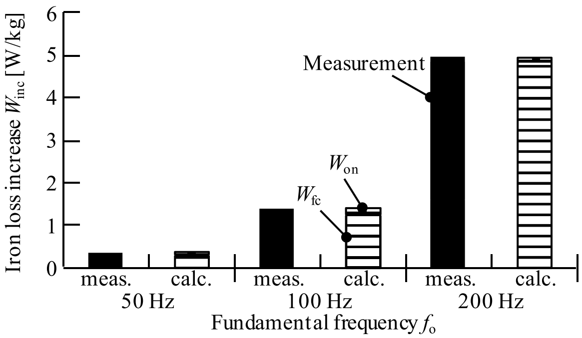

Fig. 21. Iron loss increase on each fundamental frequency ($f_c = 1$ kHz, $m = 0.5$, and $B_{\max} = 1$ T).

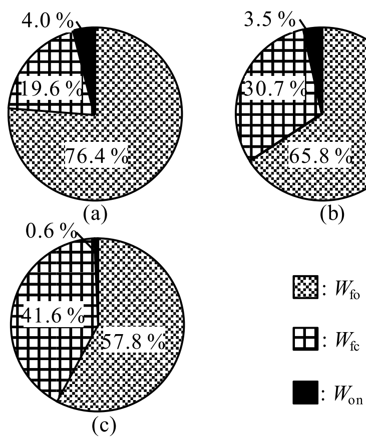

Fig. 22. Loss percentages on fundamental frequency (a) 50, (b) 100, and (c) 200 Hz ($f_c = 1$ kHz, $m = 0.5$, and $B_{\max} = 1$ T).

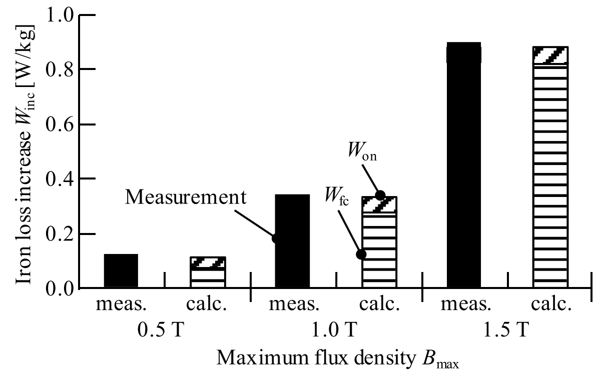

Fig. 23. Iron loss increase on each maximum flux density ($f_o = 50$ Hz, $f_c = 1$ kHz, and $m = 0.5$).

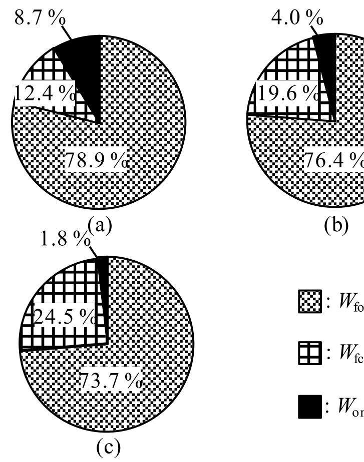

Fig. 24. Loss percentages on maximum magnetic flux density (a) 0.5, (b) 1, and (c) 1.5 T ($f_o = 50$ Hz, $f_c = 1$ kHz, and $m = 0.5$).

W_{ON} becomes small with large modulation index, because the OFF-mode time for one fundamental period becomes short when modulation index becomes large. In Fig. 20, the proportion of W_{ON} decreases when modulation index becomes large.

Next, fundamental frequency f_o or maximum magnetic flux density $B_{\max}$, which are main parameters for driving electrical machine, are changed. When f_o is changed, $B_{\max}$ is set to constant value 1 T. When $B_{\max}$ is changed, f_o is set to 50 Hz. In both cases, f_c and m are set to 1 kHz and 0.5, respectively. Figs. 21 and 22 show the iron loss increase and the proportion by variation of fundamental frequency. Each W_{fo} becomes 1.077, 2.624, and 6.734 W/kg on 50, 100, and 200 Hz, respectively. In Fig. 21, W_{ON} is almost constant with fundamental frequency, because the OFF-mode time for one fundamental period is constant. The proportion of W_{ON} becomes small on high fundamental frequency in Fig. 22. Figs. 23 and 24 show the results by variation of maximum magnetic flux density. W_{fo} is constant with 1.077 W/kg. In Fig. 23, W_{ON} increases a little when the maximum flux becomes large. To obtain large magnetic flux density, large magnetic field intensity is necessary: large current is also necessary. Therefore, since the ON-voltage shown in Fig. 9 becomes large, W_{ON} caused by ON-voltage becomes large on large magnetic flux. The proportion of W_{ON} becomes small on large magnetic flux in Fig. 24.

As a summary of those results, W_{ON} is almost constant with carrier frequency and fundamental frequency, decreases on large modulation index, and increases a little on large magnetic flux density. The proportion of W_{ON} decreases on large fundamental frequency, modulation index, and magnetic flux density. In the condition used for this paper, the percentage is up to 10%.

V. Conclusion

To clarify an influence rate of ON-voltages on iron loss under inverter excitation, the factor analysis is carried out by separating the whole iron loss into three losses: loss by ON-voltage, losses by fundamental component, and loss by inverter carrier. As a result, the loss by ON-voltage depends on modulation index and maximum flux density; hardly depends on carrier frequency and fundamental frequency. In particular, dependence for modulation index is noticeable. The proportion of the loss becomes small on large fundamental frequency, modulation index, and magnetic flux density. The percentage of the loss by ON-voltage is up to around 10% under condition used for this paper.

As a future work, we will carry out an experimental investigation and an evaluation using another magnetic material and power semiconductor.

References

[1] S. Xue *et al.*, “Iron loss model for electrical machine fed by low switching frequency inverter,” *IEEE Trans. Magn.*, vol. 53, no. 11, Nov. 2017, Art. no. 2801004, doi: 10.1109/TMAG.2017.2696360.

[2] T. Sasayama, M. Morita, and M. Nakano, “Experimental study on effect of load on iron loss of an electrical steel sheet under PWM inverter excitation,” *IEEE Trans. Magn.*, vol. 50, no. 11, Nov. 2014, Art. no. 6000504.

[3] P. Sergeant, H. Vansompel, A. Hemeida, A. Van den Bossche, and L. Dupre, “A computationally efficient method to determine iron and magnet losses in VSI-PWM fed axial flux permanent magnet synchronous machines,” *IEEE Trans. Magn.*, vol. 50, no. 8, Aug. 2014, Art. no. 8101710.

[4] M. Kawabe, T. Nomiyama, A. Shiozaki, H. Kaihara, N. Takahashi, and M. Nakano, “Behavior of minor loop and iron loss under constant voltage type PWM inverter excitation,” *IEEE Trans. Magn.*, vol. 48, no. 11, pp. 3458–3461, Nov. 2012.

[5] H. Kaihara *et al.*, “Effect of carrier frequency and circuit resistance on iron loss of electrical steel sheet under single-phase full-bridge PWM inverter excitation,” *IEEE Trans. Magn.*, vol. 48, no. 11, pp. 3454–3457, Nov. 2012.

[6] T. Shimizu and S. Iyasu, “A practical iron loss calculation for AC filter inductors used in PWM inverters,” *IEEE Trans. Ind. Electron.*, vol. 56, no. 7, pp. 2600–2609, Jul. 2009.

[7] R. Liu, C. C. Mi, and D. W. Gao, “Modeling of eddy-current loss of electrical machines and transformers operated by pulsewidth-modulated inverters,” *IEEE Trans. Magn.*, vol. 44, no. 8, pp. 2021–2028, Aug. 2008.

[8] J. Sagarduy, A. J. Moses, and F. J. Anayi, “Eddy current losses in electrical steels subjected to matrix and classical PWM excitation waveforms,” *IEEE Trans. Magn.*, vol. 42, no. 10, pp. 2818–2820, Oct. 2006.

[9] A. J. Moses and N. Tutkun, “Investigation of power loss in wound toroidal cores under PWM excitation,” *IEEE Trans. Magn.*, vol. 33, no. 5, pp. 3763–3765, Sep. 1997.

[10] A. Boglieni, O. Bottauscio, M. Chiampi, M. Pastorelli, and M. Repetto, “Computation and measurement of iron losses under PWM supply conditions,” *IEEE Trans. Magn.*, vol. 32, no. 5, pp. 4302–4304, Sep. 1996.

[11] A. Boglietti, P. Ferraris, M. Lazzari, and M. Pastorelli, “Change of the iron losses with the switching supply frequency in soft magnetic materials supplied by PWM inverter,” *IEEE Trans. Magn.*, vol. 31, no. 6, pp. 4250–4252, Nov. 1995.

[12] W. A. Roshen, “A practical, accurate and very general core loss model for nonsinusoidal waveforms,” *IEEE Trans. Power Electron.*, vol. 22, no. 1, pp. 30–40, Jan. 2007.

[13] J. Muhlethaler, J. Biela, J. W. Kolar, and A. Ecklebe, “Improved core-loss calculation for magnetic components employed in power electronic systems,” *IEEE Trans. Power Electron.*, vol. 27, no. 2, pp. 964–973, Feb. 2012.

[14] Z. Yan, C. Qimi, and Z. Junbo, “Predicting core losses under the DC bias based on the separation model,” *IEEE J. Emerg. Sel. Topics Power Electron.*, vol. 5, no. 2, pp. 833–840, Jun. 2017.

[15] K. Fujisaki and S. Liu, “Magnetic hysteresis curve influenced by power-semiconductor characteristics in pulse-width-modulation inverter,” *J. Appl. Phys.*, vol. 115, no. 17, p. 17A321, 2014.

[16] D. Kyamoari and K. Fujisaki, “Influence of power semiconductor on-voltage on iron loss of inverter-fed,” in *Proc. IEEE Power Electron. Drive Syst. (PEDS)*, Apr. 2013, pp. 840–845.

[17] S. Odawara, D. Kayamori, and K. Fujisaki, “Iron loss characteristics of electrical steel sheet under inverter excitation by using power semiconductor with extremely low on-voltage property,” (in Japanese), *IEEJ Trans. Ind. Appl.*, vol. 134, no. 7, pp. 649–655, 2014.

[18] P. Handgruber, A. Stermecki, O. Bíró, V. Goričan, E. Dlala, and G. Ofner, “Anisotropic generalization of vector Preisach hysteresis models for nonoriented steels,” *IEEE Trans. Magn.*, vol. 51, no. 3, Mar. 2015, Art. no. 7300604.

[19] P.-K. Wong, Q. Xu, C.-M. Vong, and H.-C. Wong, “Rate-dependent hysteresis modeling and control of a piezostage using online support vector machine and relevance vector machine,” *IEEE Trans. Ind. Electron.*, vol. 59, no. 4, pp. 1988–2001, Apr. 2012.

[20] S. E. Zirka, Y. I. Moroz, P. Marketos, A. J. Moses, and D. C. Jiles, “Measurement and modeling of B-H loops and losses of high silicon nonoriented steels,” *IEEE Trans. Magn.*, vol. 42, no. 10, pp. 3177–3179, Oct. 2006.

[21] M. Enokizono, “Vector magneto-hysteresis E&S model and magnetic characteristic analysis,” *IEEE Trans. Magn.*, vol. 42, no. 4, pp. 915–918, Apr. 2006.

[22] P. J. Leonard, P. Marketos, A. J. Moses, and M. Lu, “Iron losses under PWM excitation using a dynamic hysteresis model and finite elements,” *IEEE Trans. Magn.*, vol. 42, no. 4, pp. 907–910, Apr. 2006.

[23] S. Bobbio, G. Miano, C. Serpico, and C. Visone, “Models of magnetic hysteresis based on play and stop hysterons,” *IEEE Trans. Magn.*, vol. 33, no. 6, pp. 4417–4426, Nov. 1997.

[24] M. Alexandru *et al.*, “SiC integrated circuit control electronics for high-temperature operation,” *IEEE Trans. Ind. Electron.*, vol. 62, no. 5, pp. 3182–3191, May 2015.

[25] S. Rohner, S. Bernet, M. Hiller, and R. Sommer, “Modulation, losses, and semiconductor requirements of modular multilevel converters,” *IEEE Trans. Ind. Electron.*, vol. 57, no. 8, pp. 2633–2642, Aug. 2010.

[26] T. H. Kim and J. Lee, “Comparison of the iron loss of a flux-reversal machine under four different PWM Modes,” *IEEE Trans. Magn.*, vol. 43, no. 4, pp. 1725–1728, Apr. 2007.

[27] S. Odawara, K. Fujisaki, T. Matsuo, and Y. Shindo, “Evaluation of magnetic properties considering semiconductor properties by using numerical technique coupling inverter circuit analysis to magnetic analysis,” (in Japanese), *IEEJ Trans. Ind. Appl.*, vol. 135, no. 12, pp. 1191–1198, 2015.

[28] Y. Shindo, T. Miyazaki, and T. Matsuo, “Cauer circuit representation of the homogenized eddy-current field based on the Legendre expansion for a magnetic sheet,” *IEEE Trans. Magn.*, vol. 52, no. 3, Mar. 2016, Art. no. 6300504.

[29] Y. Shindo and O. Noro, “Simple circuit simulation models for eddy current in magnetic sheets and wires,” *IEEJ Trans. Fundam. Mater.*, vol. 134, no. 4, pp. 173–181, 2014.

[30] T. Miyazaki, T. Mifune, T. Matsuo, Y. Shindo, Y. Takahashi, and K. Fujiwara, “Equivalent circuit modeling of dynamic hysteretic property of silicon steel under pulse width modulation excitation,” *J. Appl. Phys.*, vol. 117, no. 17, p. 17D110, 2015.

Shunya Odawara (M’11) was born in 1987. He received the B.Eng., M.Eng., and Dr.Eng. degrees from Saga University, Saga, Japan, in 2009, 2010, and 2013, respectively.

From 2013 to 2016, he was with the Toyota Technological Institute (TTI), Aichi, Japan, as a Post-Doctoral Researcher, where he was a Commission Researcher in 2016. His current research interests include loss evaluation of magnetic material and electrical motor by inverter excitation taking account of magnetic and semiconductor property.

Keisuke Fujisaki (SM’02) was born in 1958. He received the B.Eng., M.Eng., and Dr.Eng. degrees in electronics engineering from The University of Tokyo, Tokyo, Japan, in 1983, 1986, and 1987, respectively.

In 1986, he joined Nippon Steel Corporation, Tokyo. Since 2010, he has been a Professor with the Toyota Technological Institute, Nagoya, Japan. From 2002 to 2003, he was a Visiting Professor with Oita University, Oita, Japan. From 2003 to 2009, he was a Visiting Professor with Tohoku University, Sendai, Japan. His current research interests include magnetic multiscale and electromagnetic multiphysics, including electrical motors, electromagnetic material processing, and electrical steel.